


Surface modification of new cellulose fiber extracted from *Conium maculatum* plant: a comparative study

Yasemin Seki · Ahmet Çağrı Kılınç · Ramazan Dalmis · Metehan Atagür · Serhan Köktaş  · Ali Aydın Göktaş · Erdal Çelik · Mehmet Özgür Seydibeyoğlu · Ali Bülent Önay

Received: 26 September 2017 / Accepted: 17 April 2018 / Published online: 24 April 2018
© Springer Science+Business Media B.V., part of Springer Nature 2018

Abstract This study addresses the modification and characterization of *Conium maculatum* fiber to enhance its usability as reinforcement in polymeric composite materials. The fibers were treated with alkali, silane, potassium permanganate, potassium dichromate and silicone oil, then surface chemistry (fourier transform spectroscopy and X-ray photoelectron spectroscopy), thermal stability (thermogravimetric analysis) and morpho-structure (X-ray diffraction and scanning electron microscopy) of the fibers were characterized by instrumentally. It was determined that the treatments increased hydrogen bond index and oxygen/carbon atomic ratio of the fibers. Alkali treatment had a positive impact on crystallinity index of the fiber by improving crystallite packing order following partial removal of non-cellulosic agents. The oxidation agents and the silane coupling agent reduced the crystallinity index of the fiber as a result of opening of glucopyranose rings and

the increments in the distance between the cellulose macromolecular chains, respectively. Thermal degradation temperatures of the fiber were improved after treatment and the fiber presented rougher surface after treatments that can be an advantage when used as reinforcement to enhance mechanical strength of the final composite.

Keywords *Conium maculatum* · Fiber · Surface treatment · Alkali · Composite

Introduction

Requirement for new materials particularly in aerospace, automobile, civil-engineering and manufacturing industries have been globally increased. Scientists continue their efforts to develop new materials with different features, so hybrid materials such as composites have replaced conventional materials because of superior properties and functional performance. Because of increasing awareness and sensitivity to ecologically friendly production and sustainability, bio-renewable sources such as plant fiber have received attention as alternative reinforcements of these composites. Even though they have beneficial properties such as light weight, biodegradability, non-corrosive behavior, non-toxicity, recyclability and ecologically friendly, plant fibers are not compatible with non-polar polymers due to their highly polar

Y. Seki
Department of Textile Engineering, Dokuz Eylul
University, Buca, Izmir, Turkey

A. Ç. Kılınç · R. Dalmis · S. Köktaş (✉) ·
A. A. Göktaş · E. Çelik · A. B. Önay
Department of Metallurgical and Materials Engineering,
Dokuz Eylul University, Buca, Izmir, Turkey
e-mail: serhankoktas@gmail.com

M. Atagür · M. Ö. Seydibeyoğlu
Department of Materials Science and Engineering, Izmir
Katip Celebi University, Cigli, Izmir, Turkey

character in nature (Indran et al. 2016; Ibrahim et al. 2016). Therefore, weak interfacial adhesion occurs between the fibers and non-polar polymers when used as a reinforcement material. Different approaches have been applied to plant fibers in order to enhance compatibility with polymer matrices by means of improving surface structure.

Considering previous research on surface modifications of plant fibers, it is determined that there are several chemical agents and methods used having different effect mechanisms. Alkali treatment which is commonly carried out for cellulose based fibers to remove waxy substances, natural oils and non-cellulosic components covering the fiber surface (Mwai-kambo and Ansell 2002; Cai et al. 2016). This treatment provides cleaner and rougher fiber surface which is ideal for reinforcement fibers (Orue et al. 2015). Silane coupling agents have bifunctional structures which can form chemical bridges between the fiber and the polymer in composite material (Zhou et al. 2014). In many related papers, spectroscopic analyses confirmed the condensation reaction between silane molecules and the cellulose fiber (Rachini et al. 2012). Silane treatment was revealed to change the surface topography, chemical structure and thermal degradation behaviour of the sisal fibers (Zhou et al. 2014). Treatments with silane coupling agents were revealed to increase surface hydrophobicity and to improve interfacial adhesion with the polymers (Girones et al. 2007; Orue et al. 2015). The chemical modification with oxidizing agents is another technique commonly used for cellulosic fibers (Khan et al. 2006; Zaman et al. 2010; Khan et al. 2012, 2014). Oxidation of fibers promotes surface roughness and causes fiber brittleness (Khan et al. 2012). It is also determined that oxidation agents provide more hydrophobic surface and high interfacial adhesion relatively non-polar polymers (Bulut and Aksit 2013). Additionally, another method studied for fiber treatment in terms of decreasing surface polarity includes changing the surface tension and impregnating the fibers (Torres and Cubillas 2005; Spoljaric et al. 2009). Moreover, acetylation (Diharjo et al. 2017), benzylation (Paul et al. 2008), acrylation (Gurdag et al. 2001), isocyanation (Karmarkar et al. 2007), polymer grafting on surface of the fiber (Bismarck et al. 2002) and also physical methods (Kalia et al. 2013; Kolarova et al. 2013) are studied for treatment of plant fibers.

Accordingly, the objective of this study is to modify the surface character of *Conium maculatum* fibers in order to enhance interfacial adhesion with relatively non-polar polymers when used as a reinforcement material. In the previous study, structural and morphological properties of *Conium maculatum* fibers were characterized instrumentally (Kılınç et al. 2018). According to related literature, no information has been given on surface modification of *Conium maculatum* fibers. On the other hand, although there are plenty studies about surface modifications of natural fibers originated from other plants, there are few studies in which many different surface modifications have been performed comparatively. For this purpose, *Conium maculatum* fibers were treated with alkali, silane coupling agent, potassium dichromate, potassium permanganate and silicone oil. The efficiency of the surface treatment on *Conium maculatum* fibers were investigated by Fourier transform infrared (FTIR), X-ray photoelectron spectroscopy (XPS), thermogravimetric analysis (TGA), X-ray diffraction (XRD) and scanning electron microscopy (SEM).

Experimental

Materials

The stems of locally harvested *Conium maculatum* plants from Bahadrlı village (Canakkale-TURKEY) were separated from branches and foliages. Prior to the retting process, the stems were severally washed with distilled water to remove impurities. The *Conium maculatum* fibers were extracted by the conventional water retting process. The extraction procedure was explained in details elsewhere (Kılınç et al. 2018). For surface treatment of the fibers, silicone oil, potassium dichromate, potassium permanganate and alkali were purchased from Merck Corp (USA). Tetraethoxysilane ($C_8H_{20}O_4Si$) was provided from Setas Kimya, Turkey.

Fiber treatment

Silane treatment

Prior to fiber treatment, tetraethoxysilane was hydrolyzed in 50/50% v/v ethanol/water solution with the addition of acetic acid to adjust pH 4.5–5 by

continuously stirring for 1 h at ambient temperature. Then, *Conium maculatum* fibers were added into 5% w/w hydrolyzed silane solution and kept mechanical stirring for 3 h to ensure the adsorption of the silane onto the fibers. Afterwards, the fibers were rinsed with distilled water several times to remove chemical residues. Then, the fibers were dried for 3 days at ambient temperature and then oven-dried at 80 °C (Gharbi et al. 2014; Erdogan et al. 2016).

Silicone oil treatment

Conium maculatum fibers were modified with 1% v/v silicone oil in ethanol solution at 20 °C for 30 min. Then, the fibers were oven-dried at 80 °C (Spoljaric et al. 2009).

Potassium permanganate treatment

Conium maculatum fibers were treated with 0.02% potassium permanganate aqueous solution for 30 min at room temperature. The fibers were rinsed with distilled water several times to remove chemical residues. Afterwards, the fibers were oven-dried at 100 °C and kept in a dessicator (Bulut and Aksit 2013).

Potassium dichromate treatment

Conium maculatum fibers were treated with 2.0% potassium dichromate aqueous solution for 30 min at room temperature. The fibers were rinsed with distilled water several times to remove chemical residues. Afterwards, the fibers were oven-dried at 100 °C and kept in a dessicator.

Alkali treatment

The treatment was carried out by dipping the *Conium maculatum* fibers in 5% w/v sodium hydroxide aqueous solution for 30 min at ambient temperature. Then, treated fibers were washed rinsed with distilled water with a drop of acetic acid in order to neutralize. The washed fibers were oven-dried at 80 °C (Sgriccia et al. 2008; Sinha and Rout 2009).

Characterization of the untreated and treated *Conium maculatum* fibers

FTIR analysis

FTIR spectra of the untreated and treated *Conium maculatum* fibers were obtained using a Fourier Transform Infrared spectrometer (Perkin Elmer Spectrum BX, USA). Each spectrum was recorded in the range of 600–4000 cm⁻¹ with a resolution of 2 cm⁻¹. Spectra of the samples were obtained from 25 scans.

XPS analysis

Surface chemistry of the *Conium maculatum* fibers was analyzed through X-ray photo electron spectroscopy (XPS, ThermoScientific, USA) with monochromatic Al-K α (1486.7 eV) X-ray source and a beam size of 400 nm diameter. The vacuum pressure was below 10⁻⁹ Torr during spectra data acquisition. The XPS data were acquired between 1350 and 10 eV applying energy of 150 eV and a resolution of 1 eV. 20 scans from a single point were recorded. Sample surface were sputtered with ionic Ar gas before operation.

XRD analysis

To investigate the effects of the surface treatments on fine structure *Conium maculatum* fibers, X-ray diffraction analysis was carried out by using Rigaku ULTIMA 3 (Japan)—Rint 2200/PC system with Cu-K α radiation (λ -K α 1 = 1.54 Å) and processed by MDI-Jade 7 software. Prior to analysis, the fibers were powdered in order to use in XRD stage and the measurement was recorded in 3°–60° range at 40 kV and 36 mA with a scan speed of 2°/min. To determine the crystallinity index of the *Conium maculatum* fibers, the empirical formula was used (Segal et al. 1959) (Eq. 1).

$$CI = \frac{(I_{200} - I_{am})}{I_{200}} \times 100 \quad (1)$$

where I_{200} is the peak at maximum intensity at 2 θ angle between 22° and 23° that represents the (200) lattice which is attributed to both crystalline and amorphous diffraction. I_{am} is the intensity of

diffraction of the amorphous material, which is located at a 2θ angle between 18° and 19° where the intensity is at a minimum (Seki et al. 2013).

TGA analysis

The effect of modification on thermal stability of *Conium maculatum* fibers was determined by thermogravimetric analysis. Thermogravimetric analysis (TGA) was performed by Perkin Elmer STA 8000 (USA) TG/DTA by heating from room temperature to 700°C by a heating rate of $10^\circ\text{C}/\text{min}$ under N_2 atmosphere to avoid oxidation effects.

SEM analysis

Longitudinal sections of untreated and treated *Conium maculatum* fibers were examined by JEOL-JM 6060 (Japan) model scanning electron microscope (SEM) to characterize surface morphologies. Accelerating voltage and the spot size were set to 5 kV and 40, respectively. In order to prevent electron beam charging effect, the surfaces of the fibers were coated with Au–Pd for 150 s by sputter coating.

Results and discussion

FTIR analysis

The IR spectra of untreated and treated *Conium maculatum* fibers are depicted in Fig. 1 from 4000 to 600 cm^{-1} and Table 1 lists the position of peak and its nature of bands of FTIR spectra. The spectra peaks of $3346\text{--}3331\text{ cm}^{-1}$ correspond to O–H stretching and hydrogen bonds (Paiva et al. 2007). The intensity of the peak reduced after alkali treatment. In other words, the alcohol groups in cellulose structure get reduced with the alkali treatment (Sudha and Thilagavathi 2015). This may be due to partial removal of the fatty acids which include hydroxyl groups that are involved in hydrogen bonding with the carboxyl groups (Mwaikambo and Ansell 2002). However, the other treatments increased the intensity of this peak. The increase in the intensity of this band after silane and silicone oil treatments may be due to the grafting of silane and silicone oil onto cellulose and the intermolecular condensation between adjacent adsorbed –Si–OH groups (Abdelmouleh et al. 2004). Oxidative

treatments with potassium dichromate and potassium permanganate increased the intensity of this peak possibly because of partial removal of non-cellulosic components resulting increasing number of –OH groups (Das and Chakraborty 2006). The peaks observed between 2920 and 2700 cm^{-1} were related to the C–H stretching vibration of alkyl groups in aliphatic bonds of cellulose, lignin and hemicelluloses (Orue et al. 2015). After treatment procedures, the intensity of this peak slightly increased. The peak observed at 1239 cm^{-1} indicating C–O stretching vibration of acetyl group in hemicelluloses showed diminishing intensity and further the peak 1734 cm^{-1} corresponds to carbonyl groups related to hemicellulose disappeared after alkali treatment (Rajkumar et al. 2016; Erdogan et al. 2016). Potassium permanganate and potassium dichromate treatments increased the intensity of the peak indicating the carbonyl groups probably due to the oxidation affect (Bulut and Aksit 2013). The O–H bending of water absorbed into cellulose fiber structure was located at 1617 cm^{-1} . The peak centered at 1507 cm^{-1} corresponds to C–C in plane symmetrical stretching vibration of aromatic rings present in lignin (Orue et al. 2015). The small peak at $1157\text{--}1160\text{ cm}^{-1}$ can be attributed to C–O–C asymmetric stretching (Sharma et al. 2015). The absorption band at 1034 cm^{-1} may be attributed to cyclic alcohol groups (Seki 2009). After alkali treatment, this band presented diminishing intensity whereas silane and oxidation treatment increased this band noticeably. However, after silicone-oil treatment, the major absorption peak obtained at 1019 cm^{-1} corresponds to Si–O–Si stretching vibrations (Spoljaric et al. 2009). Further, new peaks at 1259 (Si–O) and 798 (Si–C) cm^{-1} and also shoulders at 2964 (Si–O) and 865 (Si–O–Si) cm^{-1} absorption bands were introduced in the spectrum of silicone-oil treated *Conium maculatum* fibers (Matrajit et al. 2005; Jahagirdar and Tiwari 2004). These peaks can confirm formation of a polysiloxane layer on the fiber surface (Spoljaric et al. 2009).

An infrared ratio, which can also calculated from FTIR, shows hydrogen bond intensity (HBI). HBI can be calculated by the ratio of the absorption intensities of 3308 (OH stretching) and 1330 cm^{-1} (ring breathing with C–O stretching) (Carrillo et al. 2004; Oh et al. 2005; Chen et al. 2014). HBI values of the untreated and treated *Conium maculatum* fibers are given in Table 2. Considering the chain mobility and bond

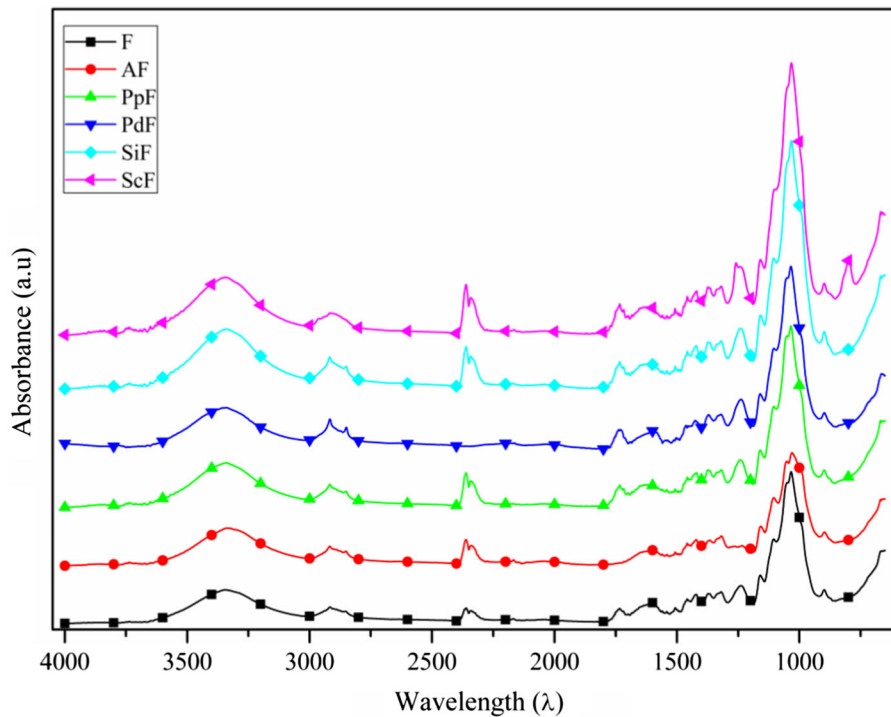


Fig. 1 FTIR spectra of the untreated and treated *Conium maculatum* fibers

Table 1 Absorption peak positions of FTIR spectra of untreated and treated *Conium maculatum* fibers. (Reproduced with permission from Ramadevi et al. 2012; Sudha and Thilagavathi 2015; Seki et al. 2016)

Bond type	F	AF	PdF	PpF	SiF	ScF
Wavenumber (cm ⁻¹)						
O–H stretching and hydrogen bonds	3346	3338	3342	3338	3345	3346
C–H stretching	2917	2918	2917	2918	2918	2916
C=O stretching of acetyl or carboxylic acid	1734	–	1738	1734	1734	1734
Absorbed H ₂ O	1617	–	–	1636	1595	–
C=C stretching of aromatic ring of lignin	1507	1508	1503	1508	1507	1507
CH bending	1370	1364	1371	1374	1374	1374
C–O–C asymmetric stretching	1160	1157	1160	1160	1158	1159
C–O stretching vibration of acetyl group in hemicellulose	1239	1234	1238	1242	1241	1259
Cyclic alcohol groups	1034	1030	1035	1034	1033	1013

F Untreated *Conium maculatum* fiber, AF alkali treated *Conium maculatum* fiber, PdF potassium dichromate *Conium maculatum* fiber, PpF potassium permanganate treated *Conium maculatum* fiber, SiF silicone oil

distance, the hydrogen-bond intensity (HBI) of cellulose is closely related to the crystal system and the degree of intermolecular regularity, that is, crystallinity, as well as the amount of bound water (Oh et al., 2005). Therefore, the crystallinity index results which are given in Table 4 are in accordance with HBI

values of the untreated and treated *Conium maculatum* fibers. All treatments performed in this study increased HBI value of the untreated *Conium maculatum* fibers by in the range of 7–20%.

Table 2 HBI values of the untreated and treated *Conium maculatum* fibers

	HBI
F	1.05
AF	1.26
SiF	1.20
PdF	1.12
PpF	1.15
ScF	1.13

XPS analysis

Table 3 lists the surface composition and C/O ratios of the untreated and treated *Conium maculatum* fibers based on XPS analysis. Figure 2 shows C1s peaks of the untreated *Conium maculatum* fiber. C1s peaks of the treated *Conium maculatum* fibers are presented in Fig. 3. As obtained from Table 3, C content slightly increased whereas O content of the untreated fiber increased by 58.3% after alkali treatment. Lignin which is one of the main components of cellulose based fibers, is partially soluble in alkali solution. Further, hemicellulose is also alkali-soluble due to its water soluble various constituents. Therefore, partial solubility of lignin and hemicellulose resulted in an increase in O/C atomic ratio of the fibers (Liu et al. 2004). The oxidation effect of potassium dichromate and potassium permanganate treatments increased O content of the fiber by 30.5 and 46.4%, respectively (Xu and Chung 2001). Silane treatment also increased oxygen content of the fibers. This is probably due to chemical structure of the tetraethoxysilane.

Apart from the other treatments, carbon content of the *Conium maculatum* fiber dramatically decreased due to the transfer of silicone atoms on the surface of the fiber. It is determined that silicone oil was well

Table 3 Surface composition (at%) and O/C ratio of the untreated and treated *Conium maculatum* fibers

	C	O	O/C	Ca	Si	N
Untreated fiber	69.2	15.1	0.22	4.25	3.91	2.53
AF	70.7	23.9	0.38	–	4.30	1.12
PdF	76.0	19.7	0.26	1.23	1.95	1.08
PpF	74.2	22.1	0.30	1.32	0.80	1.09
SiF	74.1	20.4	0.28	1.08	2.28	1.60
ScF	56.7	21.7	0.37	0.8	21.7	–

applied due to 22% content of Si atoms examined on surface of the fiber. In case of O/C atomic ratios summarized in Table 3, all treatments increased O/C ratio of *Conium maculatum* fiber. It is determined that all treatments improved surface polarity of *Conium maculatum* fibers which can enhance interfacial adhesion with more polar polymers due to the polar–polar interaction in comparison with polypropylene and polyethylene when used as a reinforcement in composite materials (Kodama et al., 1988). It is clearly seen that great proportions for the *Conium maculatum* fibers belong to C–C groups. After treatments, the chemical bonds remain almost similar but their intensity changes. After silane and oxidation treatments, O–C=O bonds were introduced on *Conium maculatum* fibers. It is also determined that C–O–C bonds were appeared on *Conium maculatum* fibers after silane, alkali and potassium permanganate treatments.

XRD analysis

Crystallinity parameters of the untreated and treated *Conium maculatum* fibers are listed in Table 4. XRD curves of *Conium maculatum* fibers are depicted in Fig. 4. The diffraction peaks at $2\theta = 22^\circ\text{--}23^\circ$ (200) and $2\theta = 16^\circ\text{--}17^\circ$ (110) indicate the typical diffractions of cellulose I (Seki et al. 2013). However, a new diffraction peak at 12.28° 2θ angles is introduced after silicone oil treatment. Therefore, it is possible to reveal that silicone oil treatment not only decreased crystallinity index of the fibers but also changed the structure. XRD results show that an increase in the crystallinity index was obtained after alkali treatment which can indicate improvement in the order of the crystallites (Mwaikambo and Ansell 2002). The crystallite packing order may be enhanced by partial removal of hemicellulose and non-cellulosic components via alkali treatment (Erdogan et al. 2016). The crystallinity of the fiber decreased after silane treatment by 3.1%. This may be due to the introduction of the silane coupling agent to the cellulose macromolecular chains. The size of aminosilane molecules is bigger than that of –OH groups, which means the distance between the cellulose macromolecular chains increased after modification (Sheltami et al. 2015). Potassium permanganate and potassium dichromate treatments decreased crystallinity index of the untreated *Conium maculatum* fiber from 66.8 to

Fig. 2 C1s peak of untreated *Conium maculatum* fiber

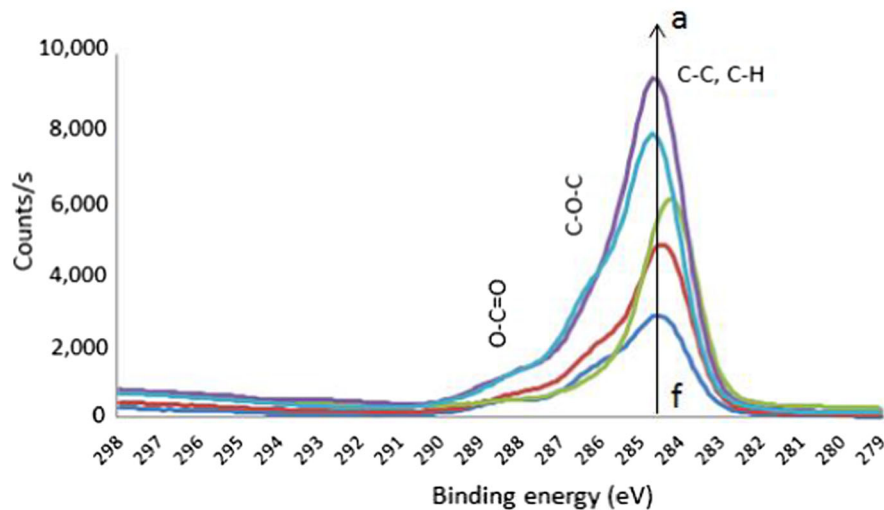
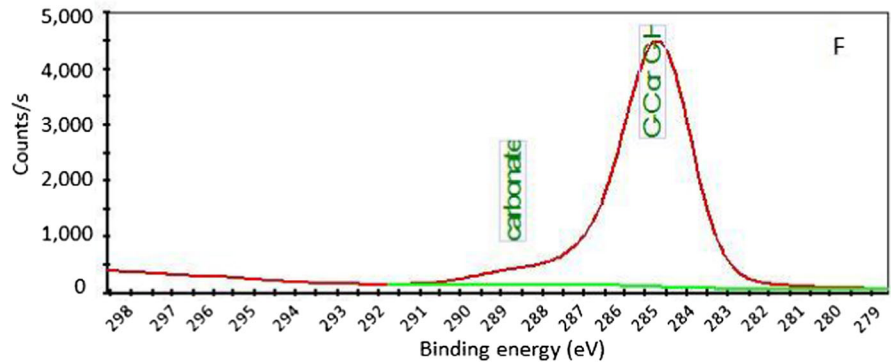


Fig. 3 C1s peaks of the treated *Conium maculatum* fiber. (a), (b), (c), (d) and (e) presents PdF, PpF, ScF, SiF and AF, respectively

Table 4 Crystallinity parameters of the untreated and treated *Conium maculatum* fibers

	F	AF	ScF	PpF	SiF	PdF
Maximum intensity at (I_{200}) 22°–23°	713	2809	1847	1399	2263	1813
Amorphous intensity (I_{am}) 18°–19°	237	726	727	482	798	694
Crystallinity index (%)	66.8	74.2	60.6	65.5	64.7	61.7

65.5% and 61.7%, respectively. The loss of crystallinity is considered to be possibly resulting from opening of glucopyranose rings and destruction of their ordered packing due to oxidation effect (Kim et al. 2000).

TGA analysis

Figure 5 shows the TG/DTG curves of the untreated *Conium maculatum* fibers. Thermogravimetric curves (TG and DTG) of the untreated and treated *Conium maculatum* fibers are shown in Figs. 6 and 7, respectively. The calorimetric results are listed in Table 5.

Except for the alkali treatment, the fibers were degraded in two main stages (~ 260 and 400 °C)

Fig. 4 XRD curves of the untreated and treated *Conium maculatum* fibers

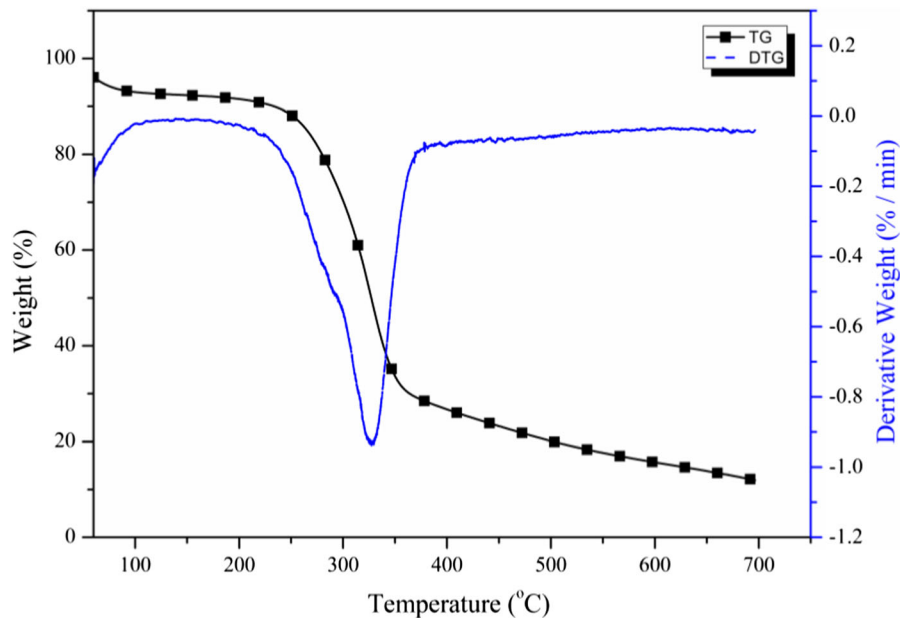
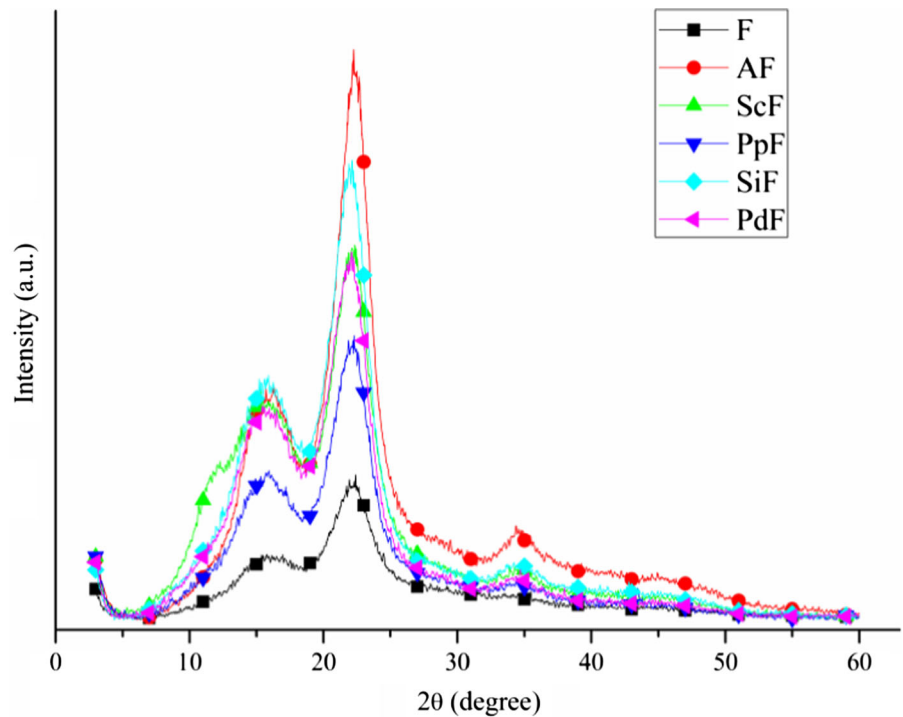


Fig. 5 TG/DTG curves of untreated the *Conium maculatum* fiber

following water vaporization which takes place between 30 and 130 °C (Melo et al. 2012). The weight loss between ~ 260 and 300 °C is related to thermal depolymerization of hemicellulose with

different weight losses of PdF (21.96%), PpF (26.86%), SiF (27.69%) and ScF (27.34%). The peaks at 336, 337.6, 343.02, 364.05, 360.25 and 361.46 °C indicate the decomposition of cellulose (Fiore et al.

Fig. 6 DTG curves of the treated *Conium maculatum* fibers

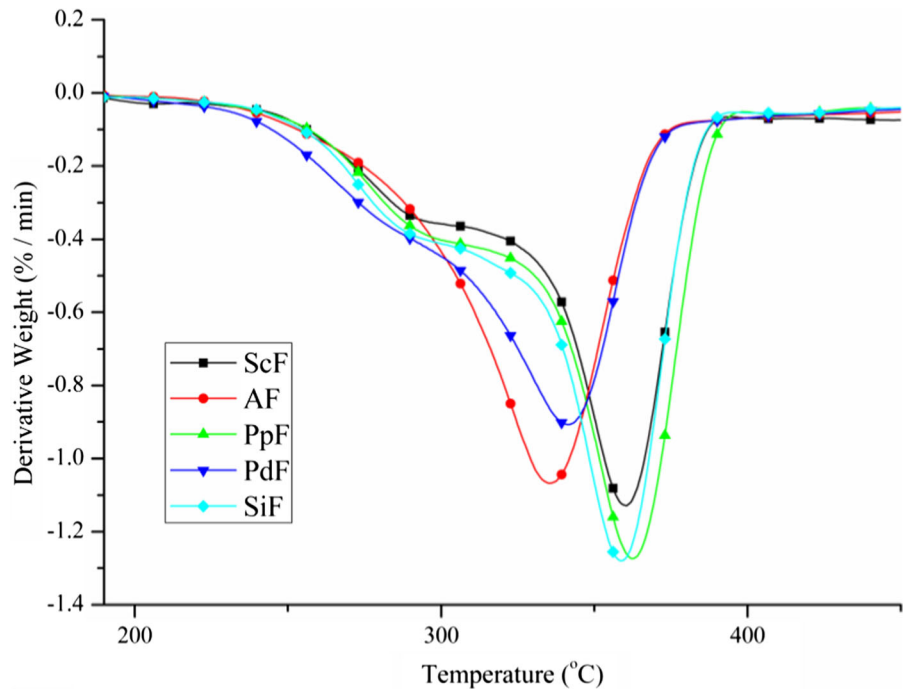
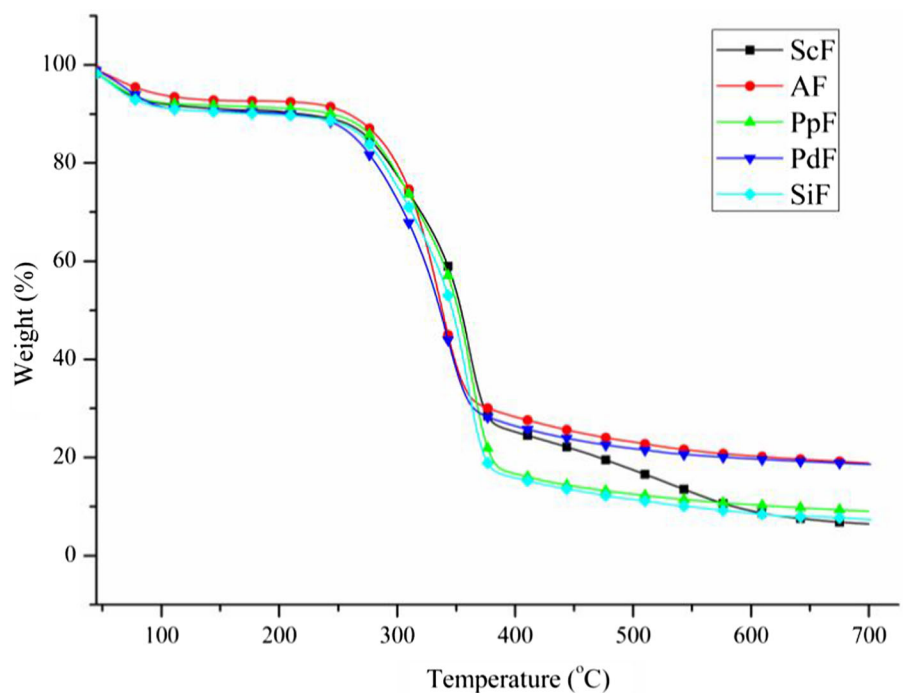


Fig. 7 TG curves of the treated *Conium maculatum* fibers



2011) corresponding weight losses of F (57.83%), AF (49.51%), PdF (56.03%), PpF (65.89%), SiF (64.44%) and ScF (58.28%), respectively. In general, the lignin decomposes in the whole temperature range (Seki

et al. 2016). It was observed that the alkali treated fibers degraded in the range of 300 and 600 °C with a single decomposition stage. This is due to the removal of hemicellulose content of the fiber. Also removal of

Table 5 Degradation temperatures of the *Conium maculatum* fibers

Fiber	T _{onset} (°C)	T _{max} (°C)
F	262.0	336.0
SiF	280.1	360.3
AF	284.1	337.6
PdF	265.1	343.0
ScF	267.7	361.5
PpF	271.6	364.1

hemicellulose content shifted the initial decomposition temperature of the fiber to higher degree (Liu et al. 2004). According to the related literature, silane treatment can enhance the thermal stability of the cellulose based fibers (Joseph et al. 2008; Eng et al. 2014; Khoathane et al. 2015; Marosi et al. 2016). Silane treatment enhanced both initial and maximum decomposition temperature of the fiber. This may be due to the formation of siloxane layer on fiber surface through the silane bridges between silanol groups of the coupling agent and the hydroxyl groups of the cellulose fiber (Li et al. 2007). These results showed that treatments retained or improved the thermal stability of fibers by improving structural order and reducing amorphous content (Melo et al. 2012).

SEM analysis

Longitudinal views of the untreated and treated *Conium maculatum* fibers are displayed in Fig. 8. As can be seen from Fig. 8a, b, untreated *Conium maculatum* fibers have a multicellular structure which longitudinally arranges with a few small pit and holes. There are also impurities on the surface of the fibers.

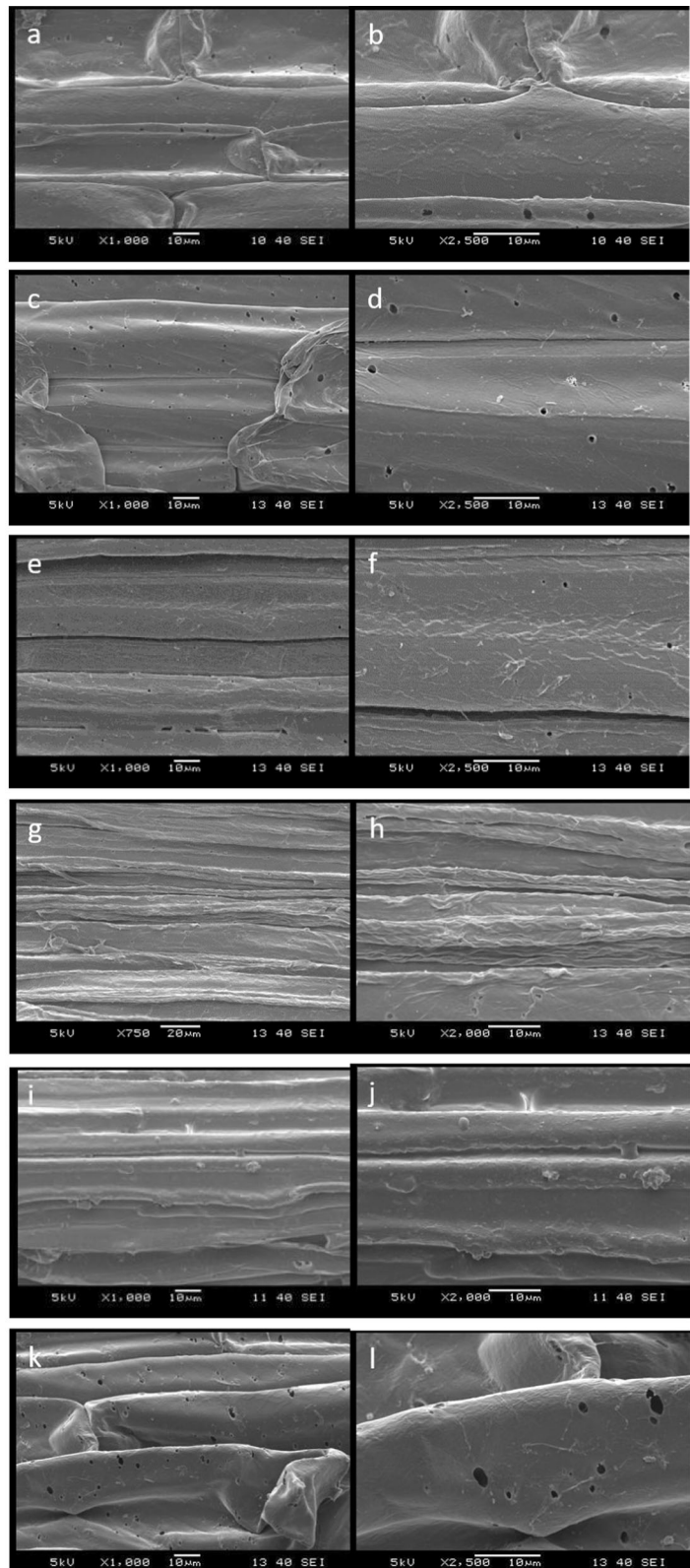
It is observed that the surface morphology of the untreated fiber changes obviously as a result of the treatments. Primarily, the least change was noticed on the fiber surface after potassium permanganate treatment (Fig. 8c, d). As a result of this treatment, it is noted that the fiber surface is cleaned from the impurities and the small ridges are seen on the fiber surface. After silane treatment, microfibers started to emerge with the gradual decay of the weak structure that holds together the fiber bundle (Fig. 8e, f). This interaction increases the surface roughness of the fiber. It can be a benefit because rougher fiber surface

enhance mechanical properties of composite materials by interlocking between fiber surface and resin interface (Sudha and Thilagavathi 2015). However, the greatest increase in roughness is achieved on the alkali treated fiber surface (Fig. 8g, h). The main reason for fibrillation is removal of hemicelluloses and lignin which are cement of the fiber body (Sudha and Thilagavathi 2015). As a result of the emerging of many fibrils on the fiber surface, the increased surface roughness can be easily detected. After silicone oil treatment, the appearance of the fiber surface is brighter, indicating that the surface is covered with the silicone oil layer (Fig. 8i, j). In addition, there are remained particles on the surface of the fiber after the related treatment. After potassium dichromate treatment, a quite different characteristic effect is observed from other treatments. As can be seen from Fig. 8k, l, the holes and pits on the fiber surface have been excessively increased. The reason for the pit and holes on the fiber surface could be the interaction of the potassium dichromate ions with the lignin components (Benyahia et al. 2016).

Conclusion

Conium maculatum fibers, alternative cellulose based fibers for polymeric composites, were treated with alkali, silane, potassium dichromate, potassium permanganate, silicone oil. All of the treatments increased HBI and O/C values of the *Conium maculatum* fibers, but the highest increments were achieved after alkali treatment due to the partial removal of lignin and hemicelluloses. Crystallinity index of the fiber increased via alkali treatment due to the enhancement in the crystallite packing by partial removal of non-cellulosic components. In contrast, silicone oil treatment did not exert a strong influence on the crystallinity index of the fiber. This may be due to the surface modification effect of silicone oil. Significant improvements in thermal degradation temperatures were observed particularly with silane and potassium permanganate treatments. The treatments alter the surface morphology of the *Conium maculatum* fibers noticeably. The treatments increased surface roughness of the fiber which can be a benefit in improving mechanical performance of the composites when used as reinforcement materials. Besides, the

Fig. 8 Longitudinal sections of **a, b** untreated, **c, d** potassium permanganate treated, **e, f** silane, **g, h** alkali treated, **i, j** silicone oil treated and **k, l** potassium dichromate treated *Conium maculatum* fibers



fiber is covered with a layer after silicone oil treatment.

References

- Abdelmouleh M, Boufi S, Belgacem MN, Duarte AP, Ben Salah A, Gandini A (2004) Modification of cellulosic fibres with functionalised silanes: development of surface properties. *Int J Adhes Adhes* 24(1):43–54
- Benyahia A, Redjem A, Rahmouni ZEA, Merrouche A (2016) Study of the mechanical properties of a composite materials: alfa fibers/unsaturated polyester. *Rom J Mater* 46(1):25–33
- Bismarck A, Arranberri-Askargorta I, Springer J, Lampke T, Wielage B, Stamboulis A, Shenderovich I, Limbach H-H (2002) Surface characterization of flax hemp and cellulose fibers; Surface properties and the water uptake behavior. *Polym Compos* 23(5):872–894. <https://doi.org/10.1002/pc.10485>
- Bulut Y, Akşit A (2013) A comparative study on chemical treatment of jute fiber: potassium dichromate potassium permanganate and sodium perborate trihydrate. *Cellulose* 20:3155–3164. <https://doi.org/10.1007/s10570-013-0049-6>
- Cai M, Takagi H, Nakagaito AN, Li Y, Waterhouse GIN (2016) Effect of alkali treatment on interfacial bonding in abaca fiber-reinforced composites. *Compos A Appl Sci Manuf* 90:589–597. <https://doi.org/10.1016/j.compositesa.2016.08.025>
- Carrillo F, Colom X, Sunol JJ, Saurino J (2004) Structural FTIR analysis and thermal characterization of lyocell and viscose-type fibres. *Eur Polym J* 40:2229–2234. <https://doi.org/10.1016/j.eurpolymj.2004.05.003>
- Chen Y, Tshabalala MA, Gao J, Stark NM, Fan Y (2014) Color and surface chemistry changes of extracted wood flour after heating at 120°C. *Wood Sci Technol* 48:137–150. <https://doi.org/10.1007/s00226-013-0582-3>
- Das M, Chakraborty D (2006) Influence of alkali treatment on the fine structure and morphology of bamboo fibers. *J Appl Polym Sci* 102(5):5050–5056
- Diharjo K, Permana A, Arsada R, Asmoro G, Herru Santosa Budiono HS, Firdaus Y (2017) Effect of acetylation treatment and soaking time to bending strength of sugar palm fiber composite. *AIP Conf Proc*. <https://doi.org/10.1063/14968302>
- Eng CC, Ibrahim NA, Zainuddin N, Ariffin H, Yunus WMZW (2014) Impact strength and flexural properties enhancement of methacrylate silane treated oil palm mesocarp fiber reinforced biodegradable hybrid composites. *Sci World J*. <https://doi.org/10.1155/2014/213180>
- Erdogan UH, Seki Y, Aydogdu G, Kutlu B, Aksit A (2016) Effect of different surface treatments on the properties of jute. *J Nat Fibers* 13(2):158–171. <https://doi.org/10.1080/15440478.2014.1002149>
- Fiore V, Valenza A, Di Bella G (2011) Artichoke (*Cynaracardunculus* L.) fibres as potential reinforcement of composite structures. *Compos Sci Technol* 71(8):1138–1144. <https://doi.org/10.1016/j.compscitech.2011.04.003>
- Gharbi A, Bel Hassen R, Boufi S (2014) Composite materials from unsaturated polyester resin and olive nuts residue: the effect of silane treatment. *Ind Crops Prod* 62:491–498. <https://doi.org/10.1016/j.indcrop.2014.09.012>
- Girones J, Mendez JA, Boufi S, Vilaseca F, Mutje P (2007) Effect of silane coupling agents on the properties of pine fibers/polypropylene composites. *J Appl Polym Sci* 103:3706–3717. <https://doi.org/10.1002/app.25104>
- Gurdag G, Guclu G, Ozgumus S (2001) Graft copolymerization of acrylic acid onto cellulose: effects of pretreatments and crosslinking agent. *J Appl Polym Sci* 80(12):2267–2272. <https://doi.org/10.1002/app.1331>
- Ibrahim ID, Jamiru T, Sadiku RE, Kupolati WK, Agwuncha SC (2016) Dependency of the mechanical properties of sisal fiber reinforced recycled polypropylene composites on fiber surface treatment fiber content and nanoclay. *J Polym Environ* 25(2):427–434. <https://doi.org/10.1007/s10924-016-0823-2>
- Indran S, Edwin Raj R, Daniel BSS, Saravanakumar SS (2016) Cellulose powder treatment on *Cissus quadrangularis* stem fiber-reinforcement in unsaturated polyester matrix composites. *J Reinf Plat Compos* 35(3):212–227. <https://doi.org/10.1177/0731684415611756>
- Jahagirdar CJ, Tiwari LB (2004) Effect of dichlorodimethylsilane on plasma treated cotton fabric. *J Phys* 62:1099–1109. <https://doi.org/10.1007/BF02705256>
- Joseph S, Sreekala MS, Thomas S (2008) Effect of chemical modifications on the thermal stability and degradation of banana fiber and banana fiber-reinforced phenol formaldehyde composites. *J Appl Polym Sci* 110:2305–2314. <https://doi.org/10.1002/app.27648>
- Kalia S, Thakur K, Celli A, Kiechel MA, Schauer CL (2013) Surface modification of plant fibers using environment friendly methods for their application in polymer composites textile industry and antimicrobial activities: a review. *J Environ Chem Eng* 1(3):97–112. <https://doi.org/10.1016/j.jece.2013.04.009>
- Karmarkar A, Chauhan SS, Modak JM, Chanda M (2007) Mechanical properties of wood–fiber reinforced polypropylene composites: effect of a novel compatibilizer with isocyanate functional group. *Compos A Appl Sci Manuf* 38(2):227–233. <https://doi.org/10.1016/j.compositesa.2006.05.005>
- Khan MA, Hassan MM, Taslima R, Mustafa AI (2006) Role of pretreatment with potassium permanganate and urea on mechanical and degradable properties of photocured coir (*Cocos nucifera*) fiber with 16-hexanediol diacrylate. *J Appl Polym Sci* 100(6):4361–4368. <https://doi.org/10.9790/5736-1005017073>
- Khan JA, Khan MA, Islam R (2012) Effect of potassium permanganate on mechanical thermal and degradation characteristics of jute fabric-reinforced polypropylene composite. *J Reinf Plast Compos* 31(24):1725–1736. <https://doi.org/10.1177/0731684412458716>
- Khan JA, Khan MA, Islam R (2014) Mechanical thermal and degradation characteristics of jute fabric-reinforced polypropylene composites: effect of potassium dichromate as oxidizing agent. *Fibers Polym* 15(11):2386–2394. <https://doi.org/10.1007/s12221-014-2386-y>
- Khoathane MC, Sadiku ER, Agwuncha CS (2015) Surface modification of natural fiber composites and their potential

- application. In: Surface modification of biopolymers, vol 370. Wiley. ISBN: 978-1-118-66955-6
- Kılınc AÇ, Koktaş S, Seki Y, Atagür M, Dalmış R, Erdogan ÜH, Göktaş AA, Seydibeyoğlu MÖ (2018) Extraction and investigation of lightweight and porous natural fiber from *Conium maculatum* as a potential reinforcement for composite materials in transportation. *Compos B Eng* 140:1–8
- Kim UJ, Kuga S, Wada M, Okano T, Kondo T (2000) Periodate oxidation of crystalline cellulose. *Biomacromolecules* 1(3):488–492. <https://doi.org/10.1021/bm0000337>
- Kodama M, Karino I, Kuramoto K (1988) Polar-polar interaction and boundary phase structure between reinforcement and matrix in a polymer composite. *Polym Plast Technol Eng* 27(1):127–153. <https://doi.org/10.1080/03602558808070104>
- Kolarova K, Vosmanska V, Rimpelova S, Svorcik V (2013) Effect of plasma treatment on cellulose fiber. *Cellulose* 20(2):953–961. <https://doi.org/10.1007/s10570-013-9863-0>
- Li X, Tabil LG, Panigrahi S (2007) Chemical treatments of natural fiber for use in natural fiber-reinforced composites: a review. *J Polym Environ* 15(1):25–33. <https://doi.org/10.1007/s10924-006-0042-3>
- Liu W, Mohanty AK, Drzal LT, Askel P, Misra M (2004) Effects of alkali treatment on the structure morphology and thermal properties of native grass fibers as reinforcements for polymer matrix composites. *J Mater Sci* 39(3):1051–1054. <https://doi.org/10.1023/B:JMISC.0000017859.63167.13>
- Marosi G, Szolnoki B, Bocz K, Toldy A (2016) Fire retardant recyclable and bio-based polymer composites. *Nov Fire Retard Polym Compos Mater Technol Adv Commer Appl*. <https://doi.org/10.1016/B978-0-08-100136-3.00005-4>
- Matrajit G, Munoz Caro GM, Dratois E, d'Hendecourt L, Deboffe D, Borg J (2005) FTIR analysis of the organics in IDPs: comparison with the IR spectra of the diffuse interstellar medium. *Astron Astrophys* 433:979–995. <https://doi.org/10.1051/0004-6361:20041605>
- Melo JDD, Carvalho LFM, Medeiros AM, Souto CRO, Paskocimas CA (2012) A biodegradable composite material based on polyhydroxybutyrate (PHB) and carnauba fibers. *Compos B Eng* 43(7):2827–2835. <https://doi.org/10.1016/j.compositesb.2012.04.046>
- Mwaikambo LY, Ansell MP (2002) Chemical modification of hemp sisal jute and kapok. *J Appl Polym Sci* 84(12):2222–2234. <https://doi.org/10.1002/app.10460>
- Oh SY, Yoo DI, Shin Y, Seo G (2005) FTIR analysis of cellulose treated with sodium hydroxide and carbon dioxide. *Carbohydr Res* 340(3):417–428. <https://doi.org/10.1016/j.carres.2004.11.027>
- Orue A, Jauregi A, Pena-Rodriguez C, Labidi J, Eceiza A, Arbelaiz A (2015) The effect of surface modifications on sisal fiber properties and sisal/poly (lactic acid) interface adhesion. *Compos B* 73:132–138. <https://doi.org/10.1016/j.compositesb.2014.12.022>
- Paiva MC, Ammar I, Campos AR, Cheikh RB, Cunha AM (2007) Alfa fibres: mechanical, morphological and interfacial characterization. *Compos Sci Technol* 67(6):1132–1138. <https://doi.org/10.1016/j.compscitech.2006.05.019>
- Paul SA, Boudenne A, Ibos L, Candau Y, Joseph K, Thomas S (2008) Effect of fiber loading and chemical treatments on thermophysical properties of banana fiber/polypropylene commingled composite materials. *Compos A Appl Sci Manuf* 39(9):1582–1588. <https://doi.org/10.1016/j.compositesa.2008.06.004>
- Rachini A, Le Troedec M, Peyratout C, Smith A (2012) Chemical modification of hemp fibers by silane coupling agents. *J Appl Polym Sci* 123:601–610. <https://doi.org/10.1002/app.34530>
- Rajkumar R, Manikandan A, Saravanakumar SS (2016) Physicochemical properties of alkali-treated new cellulosic fiber from cotton shell. *Int J Polym Anal Charact* 21(4):359–364. <https://doi.org/10.1080/1023666X.2016.1160509>
- Ramadevi P, Sampathkumar D, Srinivasa CV, Bennehalli B (2012) Effect of alkali treatment on water absorption of single cellulosic abaca fiber. *BioResources* 7(3):3515–3524
- Segal L, Creely J, Martin A, Conrad C (1959) An empirical method for estimating the degree of crystallinity of native cellulose using the X-ray diffractometer. *Text Res J* 29(10):786–794. <https://doi.org/10.1177/004051755902901003>
- Seki Y (2009) Innovative multifunctional siloxane treatment of jute fiber surface and its effect on the mechanical properties of jute/thermoset composites. *Mater Sci Eng A* 508(1–2):247–252. <https://doi.org/10.1016/j.msea.2009.01.043>
- Seki Y, Sarikanat M, Sever K, Durmuşkahya C (2013) Extraction and properties of *Ferula communis* fibers as novel reinforcement for composites materials. *Compos B Eng* 44(1):517–523. <https://doi.org/10.1016/j.compositesb.2012.03.013>
- Seki Y, Seki Y, Sarikanat M, Sever K, Durmuşkahya C, Bozaci E (2016) Evaluation of linden fibre as a potential reinforcement material for polymer composites. *J Ind Text* 45(6):1221–1238. <https://doi.org/10.1177/1528083714557055>
- Sgriccia N, Hawley MC, Misra M (2008) Characterization of natural fiber surfaces and natural fiber composites. *Compos A Appl Sci Manuf* 39(10):1632–1637. <https://doi.org/10.1016/j.compositesa.2008.07.007>
- Sharma G, Naushad M, Pathania D, Mittal A, El-Desoky GE (2015) Modification of *Hibiscus cannabinus* fiber by graft copolymerization: application for dye removal. *Desalination Water Treat* 54(11):3114–3121. <https://doi.org/10.1080/19443994.2014.904822>
- Sheltami RM, Kargarzadeh H, Abdullah I (2015) Effects of silane surface treatment of cellulose nanocrystals on the tensile properties of cellulose-polyvinyl chloride nanocomposite. *Sains Malays* 44(6):801–810. <https://doi.org/10.17576/jism-2015-4406-05>
- Sinha E, Rout SK (2009) Influence of fiber surface treatment on structural thermal and mechanical properties of jute fiber and its composite. *Bull Mater Sci* 32(1):35–76. <https://doi.org/10.1007/s12034-009-0010-3>
- Spoljaric S, Genovese A, Shanks RA (2009) Polypropylene-microcrystalline cellulose composites with enhanced compatibility and properties. *Compos A Appl Sci Manuf* 40(6–7):791–799. <https://doi.org/10.1016/j.compositesa.2009.03.011>
- Sudha S, Thilagavathi G (2015) Effect of alkali treatment on mechanical properties of woven jute composites. *J Text Inst*

- 107(6):691–701. <https://doi.org/10.1080/0040500020151061736>
- Torres FG, Cubillas ML (2005) Study of the interfacial properties of natural fibre reinforced polyethylene. *Polym Test* 24(6):694–698. <https://doi.org/10.1016/j.polymertesting.2005.05.004>
- Xu Y, Chung DDL (2001) Silane-treated carbon fiber for reinforcing cement. *Carbon* 39(13):1995–2001. [https://doi.org/10.1016/S0008-6223\(01\)00028-8](https://doi.org/10.1016/S0008-6223(01)00028-8)
- Zaman HU, Khan MA, Khan RA, Rahman MA, Das LR, Al-Mamun M (2010) Role of potassium permanganate and urea on the improvement of the mechanical properties of jute polypropylene composites. *Fibers Polym* 11(3):455–463. <https://doi.org/10.1007/s12221-010-0455-4>
- Zhou F, Cheng G, Jiang B (2014) Effect of silane treatment on microstructure of sisal fibers. *Appl Surf Sci* 292:806–812. <https://doi.org/10.1016/j.apsusc.2013.12.054>